Anisotropic diffusion-limited aggregation

M. N. Popescu,[1,2,*] H. G. E. Hentschel,[3,†] and F. Family[3,‡]
[1]*Max-Planck-Institut für Metallforschung, Heisenbergstrasse 3, D-70569 Stuttgart, Germany*
[2]*Institut für Theoretische und Angewandte Physik, Universität Stuttgart, Pfaffenwaldring 57, D-70569 Stuttgart, Germany*
[3]*Department of Physics, Emory University, Atlanta, Georgia 30322, USA*
(Received 20 July 2003; revised manuscript received 9 February 2004; published 16 June 2004)

Using stochastic conformal mappings, we study the effects of anisotropic perturbations on diffusion-limited aggregation (DLA) in two dimensions. The harmonic measure of the growth probability for DLA can be conformally mapped onto a constant measure on a unit circle. Here we map m preferred directions for growth to a distribution on the unit circle, which is a periodic function with m peaks in $[-\pi,\pi)$ such that the angular width σ of the peak defines the "strength" of anisotropy $\varkappa=\sigma^{-1}$ along any of the m chosen directions. The two parameters $(m,\varkappa)$ map out a parameter space of perturbations that allows a continuous transition from DLA (for small enough $\varkappa$) to m needlelike fingers as $\varkappa\to\infty$. We show that at fixed m the effective fractal dimension of the clusters $D(m,\varkappa)$ obtained from mass-radius scaling decreases with increasing $\varkappa$ from $D_{\mathrm{DLA}}\simeq 1.71$ to a value bounded from below by $D_{\min}=\frac{3}{2}$. Scaling arguments suggest a specific form for the dependence of the fractal dimension $D(m,\varkappa)$ on $\varkappa$ for large $\varkappa$ which compares favorably with numerical results.

DOI: 10.1103/PhysRevE.69.061403 PACS number(s): 61.43.Hv, 05.45.Df

I. INTRODUCTION

Nonequilibrium growth models leading naturally to self-organized fractal structures, such as diffusion-limited aggregation (DLA) [1], have attracted a great deal of interest in recent years, not only due to their relevance for various physical processes, for example dielectric breakdown [2], electrochemical deposition [3,4], and two-fluid Laplacian flow [5], but also because such harmonic growth leads naturally to one of the most interesting multifractal distributions found in nature [6,7].

A powerful method for studying such two-dimensional growth processes is the iterated stochastic conformal mapping [8–10], which has already been successfully applied to generate and analyze DLA [10,11] and Laplacian [12] growth patterns in two dimensions. This has opened the road to address many important questions related to pattern formation in DLA, such as the structure of the multifractal spectrum of DLA [13], and provided the first definite answers for how the hottest tips and the coldest fjords grow. Other topics that can be investigated using iterated conformal maps include the pinning transition in Laplacian growth [14], the difference between Hele-Shaw flows and DLA [15], as well as new topics such as the scaling of fracture surfaces formed during quasistatic cracking [16].

One of the important questions addressed soon after the original discovery of DLA by Witten and Sander [1] was that of the effect of the intrinsic anisotropy in lattice models on the shape and fractal dimension of the asymptotic aggregates [17–21]. For two-dimensional growth, it was shown that the result of such anisotropy in the microscopic attachment probability leads to clusters which asymptotically have the symmetry of the underlying lattice (following the argument in Ref. [17], this actually holds for $m\leqslant 6$, where m represents the coordination number of the lattice), and the fractal dimension of the resulting aggregate asymptotically approaches $\frac{3}{2}$. These results have also been confirmed in recent work which used iterated stochastic conformal mapping techniques to grow the clusters [22].

In the present work we use iterated stochastic conformal mapping techniques to study DLA with m preferred directions for growth. Although this naturally leads to anisotropic clusters, the present model is fundamentally different from the previous studies on lattice anisotropy. Our model is rather related to the existence of a large-scale imposed m-fold symmetry whose strength can be tuned. Specifically let us consider the case when the harmonic measure for DLA is weighted at angle ψ between the seed and the location for growth by a term $W(\psi;m,\sigma)$, where σ specifies the angular width of the preferred direction. Such a weighting $W(\psi;m,\sigma)\sim\exp[-\beta\mathcal{H}(\psi;m,\sigma)]$ could be due to an imposed external field or to growth on a surface which has an m-fold symmetry. An example would be dendritic growth in a strip [20] which can be argued to lie in the $m=1$ or $m=2$ universality class, the anisotropy increasing as the strip is narrowed.

The organization of the paper is as follows. In Sec. II we describe how we use conformal mapping methods together with an angle-dependent probability for growth $P(\theta;m,\varkappa)$ to study a model corresponding to a real-space weighting $W(\psi;m,\sigma)$. Here θ is the angle parametrizing the unit circle to which the boundary of the growing cluster is conformally mapped, m is the number of the privileged directions, and $\varkappa$ is an appropriate measure for the "strength" of the anisotropy. In Sec. III we present results for the morphology of the resulting patterns as a function of m and $\varkappa$ for specific choices of the modulation $P(\theta;m,\varkappa)$, and using scaling arguments we show that for large $\varkappa$ the effective fractal dimension $D(m,\varkappa)$ of the emerging clusters satisfies a scaling re-

*Electronic address: popescu@mf.mpg.de
†Electronic address: phshgeh@physics.emory.edu
‡Electronic address: phyff@emory.edu

lation. We conclude with a discussion of the results in Sec. IV.

II. MODEL AND THEORETICAL BACKGROUND

In the DLA model proposed by Witten and Sander [1], the growth of a cluster from a seed placed at the origin proceeds by irreversible attachment of random walkers released from infinity (in practice, from far away from the cluster's boundary). Thus the probability $P(s)$ for growth at any point s along the cluster boundary of total length L is a harmonic measure and can be written $P(s)=|\nabla V(s)|/\int_0^L ds'|\nabla V(s')|$, where $V(\mathbf{r})$ is a potential which outside the cluster obeys Laplace's equation $\nabla^2 V=0$ subject to the boundary conditions $V=0$ on the (evolving) boundary of the cluster and $V \sim \ln r$ as $r\to\infty$ (corresponding to a uniform source of particles far away from the cluster). In two dimensions, this formulation as a potential problem has been recently exploited for studying the time development of DLA based on conformal mapping techniques [8,10].

As discussed in detail in [8,10], the basic idea is to follow the evolution of the conformal mapping $\Phi^{(n)}(\omega)$ of the exterior of the unit circle in a mathematical ω plane onto the complement of the cluster of n particles in the physical z plane rather than directly the evolution of the cluster's boundary. The equation of motion for $\Phi^{(n)}(\omega)$ is determined recursively [see Fig. 1(a)]. With an initial condition corresponding to the unit circle in the physical plane $\Phi^{(0)}(\omega)=\omega$, the process of adding a new "particle" of constant shape and linear scale $\sqrt{\lambda_0}$ to the cluster of $(n-1)$ "particles" at a position s chosen according to the harmonic measure is performed using an elementary mapping $\phi_{\lambda,\theta}(\omega)$,

$$\phi_{\lambda,0}(\omega)=\omega^{1-a}\left\{\frac{(1+\lambda)}{2\omega}(1+\omega)\left[1+\omega+\omega\left(1+\frac{1}{\omega^2}-\frac{2}{\omega}\frac{1-\lambda}{1+\lambda}\right)^{1/2}\right]-1\right\}^a,$$

$$\phi_{\lambda,\theta}(\omega)=e^{i\theta}\phi_{\lambda,0}(e^{-i\theta}\omega), \tag{1}$$

which conformally maps the unit circle to the unit circle with a bump of size $\sqrt{\lambda}$ localized at the angular position θ [8]. The parameter a describes the shape of the elementary mapping; following the analysis in [10], we have used $a=0.66$ throughout this paper as we believe the large-scale asymptotic properties will not be affected by the microscopic shape of the added bump. As shown diagrammatically in Fig. 1(a), the recursive dynamics can than be represented as iterations of the elementary bump map $\phi_{\lambda_n,\theta_n}(\omega)$, resulting in the representation of the conformal map $z=\Phi^{(n)}(\omega)$ at the nth stage of growth as

$$\Phi^{(n)}(\omega)=\phi_{\lambda_1,\theta_1}\circ\phi_{\lambda_2,\theta_2}\circ\cdots\circ\phi_{\lambda_n,\theta_n}(\omega), \tag{2}$$

where the angle $\theta_n\in[-\pi,\pi)$ at step n is randomly chosen because the harmonic measure on the real cluster translates to a uniform measure on the unit circle in the mathematical plane, i.e.,

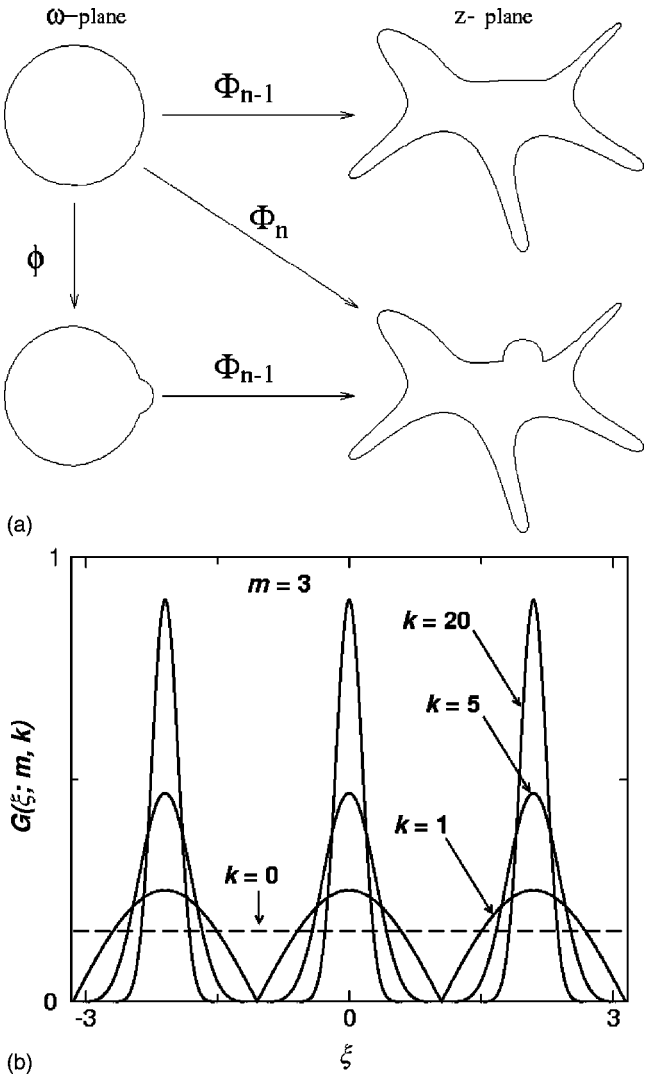

FIG. 1. (a) Diagrammatic representation of the mappings Φ and ϕ. (b) Change in shape of the probability distribution $G(\xi;m,k)$, Eq. (6), with increasing k for $m=3$.

$$P(s)ds=\frac{d\theta}{2\pi}. \tag{3}$$

Equation (3) is crucial to the successful implementation of the iterated conformal method as the highly nontrivial harmonic measure in the physical plane becomes uniform in the mathematical plane. Finally,

$$\lambda_n=\frac{\lambda_0}{|[\Phi^{(n-1)}]'(e^{i\theta_n})|^2} \tag{4}$$

is required in order to ensure that the size of the bump in the physical z plane is $\sqrt{\lambda_0}$. We note that in the composition Eq. (2) the order of iterations is inverted—the last point of the trajectory is the inner argument, therefore the transition from $\Phi^{(n)}(\omega)$ to $\Phi^{(n+1)}(\omega)$ is achieved by composing the n former maps Eq. (2) starting from a different point.

Consider the case where the existence of m preferred directions in physical space modulates the harmonic measure

at any point s on the boundary by a probability $P(\psi(s);m,\sigma)=W(\psi(s);m,\sigma)/\int_0^L ds' W(\psi(s');m,\sigma)$. Here, $\psi(s)$ is the angle parametrization of the cluster boundary in the physical space, $W(\psi;m,\sigma)$ is the modulating weight, and the m-fold periodicity implies $P(\psi+2\pi/m;m,\sigma)=P(\psi;m,\sigma)$. The important question is *if* the weighting $W(\psi;m,\sigma)$ in the real space may be represented in the form of a modulation of the constant measure in the mathematical plane $P_{\mathrm{math}}(\theta)d\theta=d\theta/2\pi$. Because the angle ψ is not invariant under the conformal map $z=\Phi^{(n)}(\omega)$, an answer to the question above is not straightforward. Considering an ensemble of clusters generated under the influence of the same modulation $P(\psi;m,\sigma)$, for each cluster of n particles ψ maps onto a different $\theta_n(\psi)$, where $\exp(i\psi)=\Phi^{(n)}(\exp(i\theta_n))/|\Phi^{(n)}(\exp(i\theta_n))|$. It is reasonable to assume that averaging over the many patterns above, an asymptotically ($n\to\infty$) scale invariant average pattern will appear. For DLA, i.e., in the absence of modulation, this pattern is a circle; in the general case, an m-fold periodic pattern with the same symmetry as the modulation is expected to appear. Therefore, we expect $\langle\theta_n(\psi)\rangle=f_m(\psi)$, where $\langle\cdots\rangle$ denotes an average over clusters, with $f_m(\psi)$ independent of n and satisfying $f_m(\psi+2\pi/m)=f_m(\psi)+2\pi/m$ (for large n) due to the symmetry of the resulting averaged pattern and to the fact that f_m is an angle [23]. It then follows that the modulated probability distribution on the unit circle leading to such m-fold symmetry patterns obeys

$$P_{\mathrm{math}}(\theta)=P(f_m^{-1}(\theta);m,\sigma)df_m^{-1}(\theta)/d\theta. \tag{5}$$

Thus, we can see that for this case $P_{\mathrm{math}}(\theta)$ is itself an m-fold periodic function on the unit circle with peaks at the preferred directions $\theta_k=2\pi k/m$.

In this paper, rather than attempting to derive a specific $P_{\mathrm{math}}(\theta)$ using Eq. (5), we shall directly assume such an m-fold periodic measure on the unit circle (which, based on the arguments above, is expected to lead to an m-fold symmetry weighting function W in the physical space) and study the clusters created using the choice $P_{\mathrm{math}}(\theta)=\mathcal{G}(\theta;m,\varkappa)d\theta$, where the parameter $\varkappa$ is an appropriate measure for the strength of selection of the preferred direction in the physical plane. The angle-dependent probability distribution on the unit circle $\mathcal{G}(\theta;m,\varkappa)$ will be normalized such that $\int_{-\pi}^{\pi}d\theta\,\mathcal{G}(\theta;m,\varkappa)=1$. Such a distribution biases the choice of the location θ, and thus s, where growth occurs as follows. At step n, the point s for the attempt of growth is chosen, as before, based on the harmonic measure, i.e., one chooses points $\theta_n\in[-\pi,\pi)$ on the unit circle with uniform distribution. But growth at s is only allowed with a probability $\mathcal{G}(\theta_n;m,\varkappa)$. If the attempt is rejected, then the previous sequence is repeated until a successful trial occurs. It thus follows that a natural choice for the parameter $\varkappa$ is the inverse of the width of the peaks of $\mathcal{G}$ since the larger $\varkappa$ is, i.e., the narrower the peaks of $\mathcal{G}$ are, the stronger is the angular selectivity. We note that obviously $\mathcal{G}(\theta;m,\varkappa)=\mathrm{const}$ corresponds to usual DLA, while an explicit dependence on θ models the existence of privileged directions. Therefore, the pair $(m,\varkappa)$ defines a two-dimensional parameter space for the analytic study of applied anisotropy to DLA.

Because at this stage we are interested in the general features of such a model of anisotropic growth, and not in trying to model a specific physical system, we shall make for $\mathcal{G}(\theta;m,\varkappa)$ the simple choice

$$G(\theta;m,k)=\frac{1}{C(k)}\left|\cos\left(\frac{m}{2}\theta\right)\right|^k,$$

$$\theta\in[-\pi,\pi),m\in\mathbb{N},k\in\mathbb{R}_+, \tag{6}$$

where

$$C(k)=\frac{4\sqrt{\pi}\,\Gamma\left(\frac{3}{2}+\frac{k}{2}\right)}{(1+k)\quad\Gamma\left(1+\frac{k}{2}\right)}$$

is the normalization constant (note that it does not depend on m). It is easy to see that $G(\theta;m,k)$ defined above has all the key properties required: for $m>0$ it is a periodic function of θ of principal period $2\pi/m$, and thus the number m of peaks of $G(\theta;m,k)$ in $[-\pi,\pi)$ corresponds to the number of privileged directions; obviously, for this particular choice both $k=0$ independent of m and $m=0$ independent of k correspond to isotropic DLA growth. At given m, the exponent $k>0$ allows the continuous tuning of the width and height of the peaks, i.e., the larger k is, the narrower and higher are the peaks of $G(\theta;m,k)$ [see Fig. 1(b)]. Thus in this case k is also a good measure for the "strength" of selectivity, and we shall use either k or $\varkappa$ (which is uniquely determined by m and k, see cf. Sec. III) as the "anisotropy strength."

Though the choice given by Eq. (6) is arbitrary, we believe that because of universality the key features will be independent of the specific form of the function $\mathcal{G}(\theta;m,\varkappa)$, and thus most of the results presented in the next section will refer to $G(\theta;m,k)$. However, as a simple check we have also tested a significantly different choice for $\mathcal{G}(\theta;m,\varkappa)$,

$$\tilde{G}(\theta;m,\varepsilon)=\frac{1}{m\varepsilon}\begin{cases}1, & \theta\in\left[\frac{2\pi}{m}j-\frac{\varepsilon}{2},\frac{2\pi}{m}j+\frac{\varepsilon}{2}\right]\cap[-\pi,\pi),j\in\mathbb{N}\\ 0 & \text{otherwise},\end{cases} \tag{7}$$

i.e., the union of m rectangular, equidistant peaks of width $\varepsilon\leqslant 2\pi/m$ (thus decreasing ε corresponds to increased angular selectivity). In this case, the width ε is independent of $\dot{m}$ (in contrast to the choice G above), the limiting case of DLA growth is obtained for $\varepsilon=2\pi/m$, and $\varkappa=\varepsilon^{-1}$ is obviously the natural choice for the "anisotropy strength."

III. RESULTS AND DISCUSSION

The model described in Sec. II was simulated as follows. The parameter $\lambda_0=10^{-3}$ was fixed because it is just setting the microscopic area of an added "particle." Considering for the moment the modulation G, Eq. (6), for fixed m and k, the

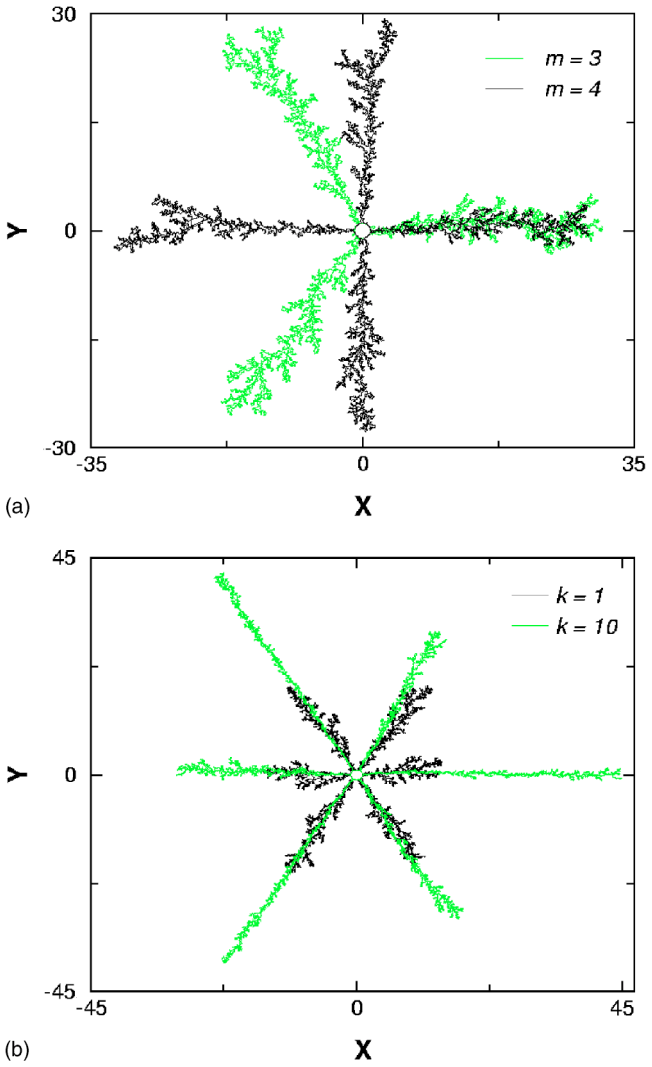

FIG. 2. (Color online) Typical clusters (size $N=20\,000$) grown using the modulation $G(\theta;m,k)$ with (a) $m=3$, 4, fixed $k=3$, and (b) fixed $m=6$, but different values for k, $k=1$, and $k=10$, respectively.

growth step n proceeds by selecting at random (uniform probability) an angle $\theta\in[-\pi,\pi)$, then comparing $G(\theta;m,k)$ with a random number r uniformly distributed in $[0,1/C(k))$; if $r<G(\theta;m,k)$, then $\theta_n=\theta$, λ_n follows from Eq. (4), and the new map Φ_n follows from Eq. (2); if not, the previous sequence is repeated until a successful trial occurs. All the averages mentioned below were done over 100 clusters grown up to size $N=20\,000$. A similar procedure has been applied in the case of the modulation $\tilde{G}$, Eq. (7), the only difference being that in this case the random number r is chosen uniformly distributed in $[0,m\varepsilon)$ (for fixed m and ε).

An example of clusters with different symmetries (i.e., different values m) grown using the modulation G is shown in Fig. 2(a), while Fig. 2(b) depicts the morphology with increasing anisotropy "strength" (i.e., different values k at fixed m).

It can be seen that the bias introduced by the distribution $G(\theta;m,k)$ is indeed producing clusters with the corresponding m-fold symmetry and that it is very effective: even for small values k, the clusters in Fig. 2(a) show a clear three-fold, and fourfold symmetry, respectively. Increasing k (the strength of the anisotropy) leads to a significant reduction in the branched structure of the cluster, thus in the thickness of the surviving branches, as shown in Fig. 2(b). Similar results have been obtained for all the values $2\leqslant m\leqslant 7$ and $1\leqslant k\leqslant 80$ that have been tested, and similar conclusions hold for the case $\tilde{G}(\theta;m,\varepsilon)$ for the tested values $2\leqslant m\leqslant 6$ and $0.1\leqslant\varepsilon\leqslant 2\pi/m$.

The results shown in Fig. 2 suggest that the resultant patterns have a fractal morphology that depends on m and k, and in order to characterize these shapes we shall focus on the effective fractal dimension $D(m,k)$ obtained from the mass-radius scaling. Following the arguments in Ref. [10], the coefficient $F_1^{(n)}=\Pi_{i=1}^{n}(1+\lambda_i)^a$ in the Laurent expansion of $\Phi^{(n)}$,

$$\Phi^{(n)}(\omega)=F_1^{(n)}\omega+F_0^{(n)}+F_{-1}^{(n)}\omega^{-1}+F_{-2}^{(n)}\omega^{-2}+\cdots, \qquad (8)$$

is a typical length scale of the cluster; thus, a natural choice for the radius of the n-particle cluster is $R\sim F_1^{(n)}$. Assuming that for $n\gg 1$ a scaling law of the form

$$F_1^{(n)}\sim n^{1/D(m,k)} \qquad (9)$$

is found, the effective fractal dimension of the cluster can be extracted from a power-law fit to the numerical data. We note in passing that this scaling law was used in Ref. [10] as a very convenient way to measure the fractal dimension of the growing DLA cluster. As we have anticipated, for all the values m and k the numerical results for the average coefficient $F_1^{(n)}$ show a power-law dependence on the size n, an example being shown in Fig. 3(a), and the results $D(m,k)$ obtained from the power-law fit to the data in the range $n\geqslant 10^3$ are shown in Fig. 3(b).

It can be seen that $D(m,k)$ decreases with increasing k at fixed m (and with increasing m at fixed k), and there is a certain tendency for saturation at large k. We note that, as expected, $D(m,0)\simeq D_{\mathrm{DLA}}$ and that the curves $D(m,k)$ are all above the expected lower limit $D_{\min}=3/2$ [17]. An exception is the case $m=7$ (results not shown), where for large k the values $D(7,k\gg 1)\simeq 1.45$ are somewhat below $D_{\min}$, but this is most probably due to either insufficient statistics (too few clusters), as suggested also by the noisiness of the $D(m,k)$ curves, or to the fact that in this particular case the size $N=20\,000$ is not sufficient to obtain an asymptotic cluster. Again, similar results hold for the case in which the modulation $\tilde{G}(\theta;m,\varepsilon)$ has been used, the only difference being that now $D(m,\varepsilon=2\pi/m)\simeq D_{\mathrm{DLA}}$ replaces the relation $D(m,k=0)\simeq D_{\mathrm{DLA}}$ above.

In order to understand these results theoretically we shall use a simple argument, following Ref. [17], based on the assumptions that (a) for large $\varkappa$ the growth of the cluster occurs mainly at the tips of the m principal branches, and (b) the envelope of the *average* cluster can be approximated by m diamond shaped polygons, like the one shown in Fig. 4(a), of opening angles γ and β (in general, these angles depend on both m and $\varkappa$) and with edges of lengths in the order of R (the radius of the cluster).

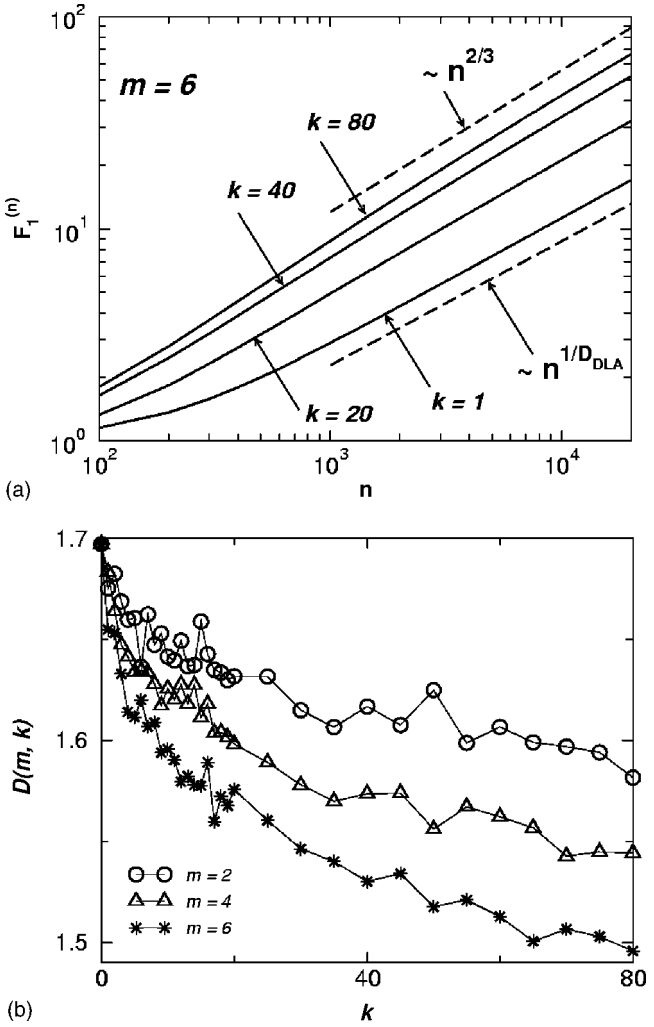

FIG. 3. (a) Average $F_1^{(n)}$ as a function of n for clusters grown with $k=1$, 10, 40, and 80, respectively, and fixed $m=6$ (log-log plot). Also shown (dashed lines) are both the limit case $F_1^{(n)} \sim n^{1/D_{\mathrm{DLA}}}$ (DLA cluster), where $D_{\mathrm{DLA}}=1.71$, and the proposed lower bound for anisotropic DLA growth, $F_1^{(n)} \sim n^{1/D_{\min}}$, where $D_{\min}=3/2$ [17]. (b) The effective fractal dimension $D(m,k)$, obtained from $F_1^{(n)} \sim n^{1/D(m,k)}$, as a function of k at fixed m. The points represent the measured values, the lines are just a guide to the eye. The results in both (a) and (b) correspond to the modulation $G(\theta;m,k)$.

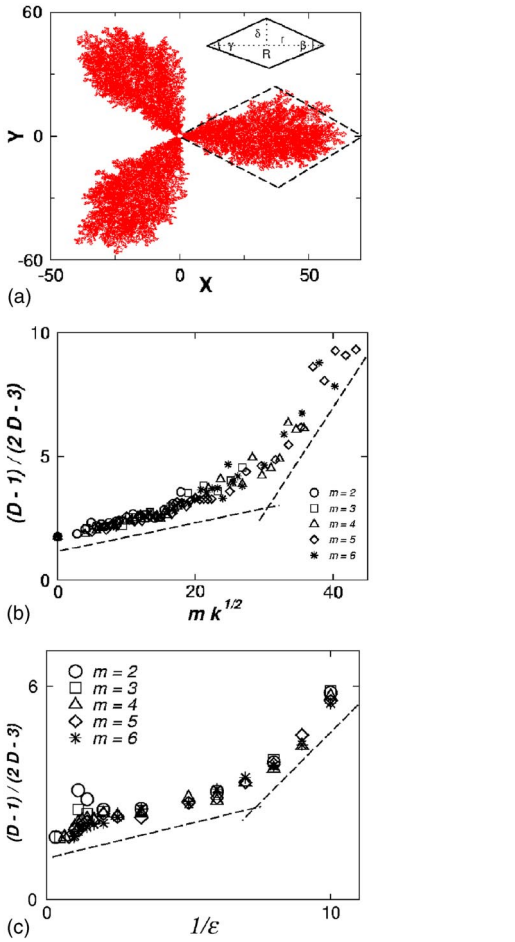

FIG. 4. (Color online) (a) Superposition of 10 different clusters of size $N=10^5$ grown with the modulation $G(\theta;m,k)$, the same $m=3$ and $k=1$, but different sequences of random numbers. The dotted diamond around the arm centered at $\psi=0$ shows the approximation for the envelope of one arm of the cluster, and the drawing in the upper right corner shows schematically the geometry of the diamond. (b),(c) Numerical results for $(D-1)/(2D-3)$ as a function of the scaling variable $\varkappa=m\sqrt{k}$ (for modulation function G) and $\chi=\varepsilon^{-1}$ (for modulation function $\tilde{G}$), respectively. The dashed lines are just a guide to the eye for the linear behavior in the range of small and large values of $\varkappa$, respectively.

Under these assumptions, the rate of growth can be written as [17]

$$dN/dR \sim R^{\pi/(2\pi-\beta)}. \tag{10}$$

Because the left-hand side of Eq. (10) is $\sim R^{D(m,\varkappa)-1}$, once the angle $\beta(m,\varkappa)$ is known, $D(m,\varkappa)$ can be determined from

$$D(m,\varkappa) = 1 + \frac{\pi}{2\pi - \beta(m,\varkappa)}. \tag{11}$$

Simple geometry [see the schematic drawing in the top right corner of Fig. 4(a)] allows one to write [under the assumption that the angles $\gamma(m,\varkappa)$ and $\beta(m,\varkappa)$ are small, which is certainly true for large $\varkappa$ and m],

$$\frac{\gamma}{2} = \frac{\delta}{R-r}, \quad \frac{\beta}{2} = \frac{\delta}{r} \Rightarrow \beta = \frac{R-r}{r}\gamma. \tag{12}$$

On the other hand, following the arguments in Sec. II, the opening angle γ is determined by the decay of the probability for growth $\mathcal{G}(\theta;m,\varkappa)$, and therefore it can be estimated as being equal to the width of the peak of the distribution. For $\tilde{G}$, this is simply ε, and thus in this case $\varkappa=1/\varepsilon=1/\gamma$. For the case of the modulation G, working with the peak centered at $\theta=0$, assuming large k and small γ, the width at half peak probability $(\theta=\gamma/2)$ is given by $1/2 \approx [1-(m\gamma/4)^2/2]^k \approx 1-k(m\gamma/4)^2/2$. Thus, in this case $\gamma(m,k) \approx 4/m\sqrt{k}$ and a good choice for $\varkappa$ is $\varkappa=m\sqrt{k}$.

From Eq. (12) it then follows that

$$\beta(m,\varkappa) \simeq \frac{(R-r)}{r\varkappa} = \frac{C_1}{\varkappa}, \tag{13}$$

where C_1 is a constant of $O(1)$. Combining Eqs. (11) and (13), one thus obtains the following scaling relation for the fractal dimension:

$$\frac{D(m,\varkappa)-1}{2D(m,\varkappa)-3} = \frac{\pi}{C_1}\varkappa. \tag{14}$$

Note that it is immediately apparent from Eq. (14) that $D_{\min}=\frac{3}{2}$, while for large $\varkappa$ the ratio $(D-1)/(2D-3)$ should be a linear function of the product $m\sqrt{k}$ *only*, provided $m\sqrt{k} \gg 1$ in the case of the modulation G, and a linear function of ε^{-1} *only* (independent of m) in the case of the modulation $\tilde{G}$, respectively. This prediction can be tested against the numerical results. As shown in Figs. 4(b) and 4(c), the data collapse is excellent in both cases and the function is indeed linear when $\varkappa \gg 1$. Surprisingly, the scaling predicted by Eq. (14) seems to hold down to quite small values of $\varkappa$, although these results are beyond the scope of our scaling arguments.

IV. CONCLUSIONS

Using iterated stochastic conformal maps, we have studied the patterns emerging from a model of anisotropic (in the sense of the existence of privileged radial directions for growth) diffusion-limited aggregation in two dimensions. In our model, the anisotropy was introduced via a probability distribution for growth with a number m of peaks in $[-\pi,\pi)$, the width of a peak being a tunable parameter that allows a continuous transition from isotropic DLA growth to anisotropic clusters. We have shown numerical evidence that at fixed m the effective fractal dimension of the clusters $D(m,\varkappa)$ obtained from the mass-radius scaling decreases with increasing anisotropy strength $\varkappa$ from D_{DLA} to values bounded from below by $D_{\min}=\frac{3}{2}$. Using simple approximations (supported by numerical results) for the envelope of the cluster and general scaling arguments, we have derived a scaling law involving $D(m,\varkappa)$ and successfully tested it against numerical results.

Although the model we have proposed is very simple, it has the advantage that it seems to capture most of the general features of an anisotropic growth process while still allowing for an analytical treatment (to a certain degree). Finally, we note here that a system for which the proposed geometry may be easily experimentally achieved is the growth of bacterial colonies. For such a case, the radial anisotropy can be experimentally obtained through the addition of nutrients along the privileged directions, and controlled through the excess concentration of nutrients along these directions with respect to the rest of the substrate. For the data analysis, the parameter m can be easily determined by visual inspection of the experimental clusters (if it is not *a priori* known), while the anisotropy strength $\varkappa$ can be determined by measuring the angular opening γ of a branch (care must be taken because at large $\varkappa$, i.e., where our scaling arguments apply, this angular opening is expected to be very small). Such an experiment would allow a direct testing of all our numerical and analytical predictions.

ACKNOWLEDGMENTS

This work has been supported by the Petroleum Research Fund. M.N.P. would like to thank the Physics Department at Emory University for the very warm hospitality during the visit when part of this work was done.

[1] T. A. Witten, Jr. and L. M. Sander, Phys. Rev. Lett. **47**, 1400 (1981).
[2] L. Niemeyer, L. Pietronero, and H. J. Wiesmann, Phys. Rev. Lett. **52**, 1033 (1984).
[3] R. M. Brady and R. C. Ball, Nature (London) **309**, 225 (1984).
[4] M. Matsushita, M. Sano, Y. Hayakawa, H. Honjo, and Y. Sawada, Phys. Rev. Lett. **53**, 286 (1984).
[5] L. Paterson, Phys. Rev. Lett. **52**, 1621 (1984).
[6] H. G. E. Hentschel and I. Procaccia, Physica D **8**, 435 (1983).
[7] T. C. Halsey, P. Meakin, and I. Procaccia, Phys. Rev. Lett. **56**, 854 (1986).
[8] M. B. Hastings and L. S. Levitov, Physica D **116**, 244 (1998).
[9] M. B. Hastings, Phys. Rev. E **55**, 135 (1997).
[10] B. Davidovitch, H. G. E. Hentschel, Z. Olami, I. Procaccia, L. M. Sander, and E. Somfai, Phys. Rev. E **59**, 1368 (1999).
[11] B. Davidovitch and I. Procaccia, Phys. Rev. Lett. **85**, 3608 (2000).
[12] F. Barra, B. Davidovitch, A. Levermann, and I. Procaccia, Phys. Rev. Lett. **87**, 134501 (2001).
[13] M. H. Jensen, A. Levermann, J. Mathiesen, and I. Procaccia, Phys. Rev. E **65**, 046109 (2002).
[14] H. G. E. Hentschel, M. N. Popescu, and F. Family, Phys. Rev. E **65**, 036141 (2002).
[15] H. G. E. Hentschel, A. Levermann, and I. Procaccia, Phys. Rev. E **66**, 016308 (2002).
[16] F. Barra, H. G. E. Hentschel, A. Levermann, and I. Procaccia, Phys. Rev. E **65**, 045101 (2002).
[17] R. C. Ball, R. M. Brady, G. Rossi, and B. R. Thompson, Phys. Rev. Lett. **55**, 1406 (1985); R. C. Ball, Physica A **140**, 62 (1986).
[18] P. Meakin, in *Phase Transitions and Critical Phenomena*, edited by C. Domb and J. Lebowitz (Academic, New York, 1988), Vol. 12.
[19] J. P. Eckmann, P. Meakin, I. Procaccia, and R. Zeitak, Phys. Rev. A **39**, 3185 (1989); Phys. Rev. Lett. **65**, 52 (1990).
[20] A. Arneodo, F. Argoul, Y. Couder, and M. Rabaud, Phys. Rev. Lett. **66**, 2332 (1991).
[21] B. K. Johnson and R. F. Sekerka, Phys. Rev. E **52**, 6404 (1995).
[22] M. G. Stepanov and L. S. Levitov, Phys. Rev. E **63**, 061102 (2001).
[23] In principle, f_m is defined up to an additive constant; this can be fixed by specifically requiring that at the fingertips $j=0,1,2,\ldots,m-1$ of the pattern one has $f_m(2\pi j/m)=2\pi j/m$.